JAAS

Accepted Manuscript

This is an *Accepted Manuscript*, which has been through the Royal Society of Chemistry peer review process and has been accepted for publication.

Accepted Manuscripts are published online shortly after acceptance, before technical editing, formatting and proof reading. Using this free service, authors can make their results available to the community, in citable form, before we publish the edited article. We will replace this *Accepted Manuscript* with the edited and formatted *Advance Article* as soon as it is available.

You can find more information about *Accepted Manuscripts* in the Information for Authors.

Please note that technical editing may introduce minor changes to the text and/or graphics, which may alter content. The journal's standard Terms & Conditions and the Ethical guidelines still apply. In no event shall the Royal Society of Chemistry be held responsible for any errors or omissions in this *Accepted Manuscript* or any consequences arising from the use of any information it contains.

ROYAL SOCIETY OF CHEMISTRY

www.rsc.org/jaas

A table of contents entry

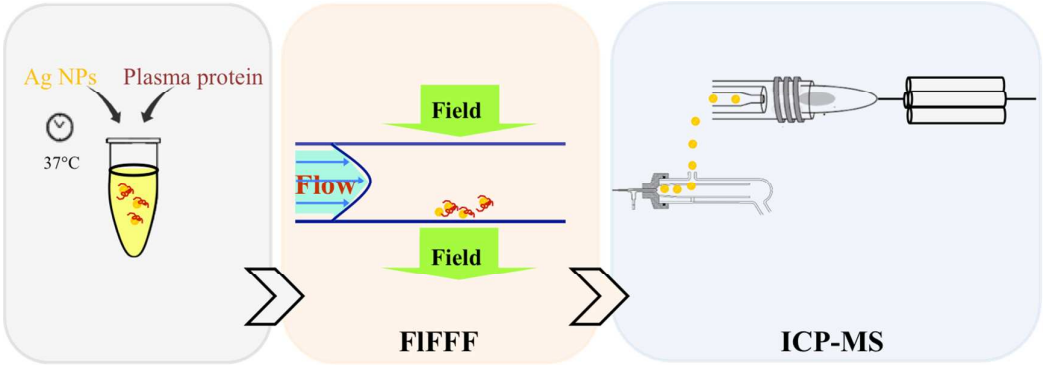

Use of FlFFF-ICP-MS for observation of protein-AgNPs binding and evaluation of the binding stoichiometry

Investigation of silver nanoparticles and plasma protein association using flow field-flow fractionation coupled with inductively coupled plasma mass spectrometry (FlFFF-ICP-MS)

Panida Wimuktiwan, Juwadee Shiowatana, and Atitaya Siripinyanond*

Department of Chemistry and Center for Innovation in Chemistry, Faculty of Science, Mahidol University, Rama VI Road, Bangkok 10400, Thailand Fax: +662-354-7151; Tel: +662-201-5195; E-mail: atitaya.sir@mahidol.ac.th

Abstract

Flow field-flow fractionation (FlFFF) with on-line inductively coupled plasma mass spectrometer (ICP-MS) was employed for investigation of protein-silver nanoparticles (AgNPs) association. In this work, bovine serum albumin (BSA), globulin, and fibrinogen were the model proteins studied. AgNPs were prepared by reduction of silver nitrate using tannic acid as reducing and stabilizing agent. Various sizes (2.6, 10, and 26 nm) were obtained depending on the pH condition during particle preparation. The apparent association constants between BSA and AgNPs of various sizes were determined. Then, various concentrations of AgNPs of 2.6 nm were incubated with plasma proteins, i.e., albumin of 2.6 x 10^{-1} M; globulin of 3.1 x 10^{-2} M; and fibrinogen of 2.9 x 10^{-3} M, at 37 °C for investigation of protein-AgNPs association. Factors influencing protein-AgNPs association were investigated including effect of incubation time and effect of AgNPs concentration. Association between protein and AgNPs increased as incubation time and concentration of

AgNPs increased. Further, the binding stoichiometry between BSA and AgNPs was determined to be approximately 1 : 5 x 10^{-7}.

Introduction

Many consumer products nowadays are claimed to contain engineered nanoparticles. Owing to its strong antimicrobial activity, silver nanoparticles (AgNPs) have been used in several applications, such as food packing materials; textile; cosmetic; household items; and wound dressing. However, the wide usage of AgNPs increases the possibility for these nanomaterials to enter into environment and human body. Human exposure to AgNPs can be from various routes, including ingestion; inhalation; dermal contact; and through therapeutic applications [1, 2].

Some researchers reported different transdermal penetration rates of AgNPs through the intact and damaged skins, which were controlled by intrinsic parameters of the skin [3]. Once entering the body, AgNPs were rapidly in contact with biological fluids such as saliva, mucus, lung lining fluid, and plasma protein [4, 5]. Therefore, the assessment of the interactions between AgNPs and plasma proteins is a very important issue. Considering the plasma proteins, the majority is albumin (55%), followed by globulin (38%) and fibrinogen (7%). Various analytical techniques were exploited to examine plasma protein-nanoparticles association in order to gain an insight into the binding between plasma proteins and AgNPs. Those techniques include ultraviolet-visible spectroscopy (UV-Vis) [6], fluorescence spectroscopy [7], dynamic light scattering (DLS) [8], atomic force microscopy (AFM) [9], and size exclusion chromatography (SEC) [10]. In this work, we proposed the use of flow field-flow fractionation (FlFFF) online with inductively coupled plasma mass spectrometry (ICP-MS) as an alternative technique for investigation of AgNPs-plasma protein association.

This hyphenated technique has been successfully applied to examine freshwater oligochaete exposure to AgNPs [11], study the effects of particle size and the coating on the bioaccumulation and depuration of AgNPs within the gut cavities of aquatic invertebrates [12], investigate the effect of UV irradiation on the stability of AgNPs [13], analyze AgNPs in chicken meat [14], and examine the association of AgNPs with HepG2 cells [15].

The aim of this work was to apply a conventional symmetrical flow field-flow fractionation (FlFFF) with online inductively coupled plasma mass spectrometry (ICP-MS) for investigation of plasma protein-silver nanoparticles (AgNPs) association. Plasma proteins studied herein included bovine serum albumin (BSA), globulin, and fibrinogen. The key parameters affecting the association between plasma proteins and AgNPs were examined, including incubation time and AgNPs concentration. The novel finding from this technique also includes the information on stoichiometric binding between AgNPs and BSA.

Experimental

Instrumentation

A symmetrical FlFFF system (Model PN-1201-FO, Postnova Analytics, Landsberg, Germany) equipped with a 1,000 Da molecular weight cut-off regenerated cellulose acetate membrane (Postnova) was used. The geometry of the FlFFF channel is 27.7 cm long, 2.0 cm wide, and 0.0254 cm thick. Sample volume of 20 µL was introduced into FlFFF via the Rheodyne® injector valve. Two high pressure liquid chromatography (HPLC) pumps (Model PN 2101, Postnova Analytics, Germany) were used to regulate the channel flow and the cross flow, respectively. In our experiment, a channel flow was set at 1 mL min^{-1} and a cross flow of 2 mL min^{-1} was used. After fractionation, the effluent was directed through a

UV detector (Model Water 2487 Dual λ Absorbance Detector, Waters, Milford, MA, USA) which was set at 280 nm for detection of the plasma proteins. The UV detector outlet was coupled to an ICP-MS instrument (Sciex/Elan 6000, PerkinElmer Instruments, Shelton, CT, USA) using a cross-flow nebulizer with 50-cm poly (tetrafluoroethylene) tubing (PTFE, 0.58 mm id). The eluted fraction from FlFFF was introduced into the ICP-MS sample introduction system for further determination of element. Both silver isotopes (^{107}Ag and ^{109}Ag) were monitored and an integration dwell time of 25 ms was set for each isotope. The total number of readings per replicate was chosen such that data were collected for the entire fractograms. To assure no drift of instrument, 20 µg L^{-1} AgNPs was used for checking the stability of the signal once after every five run. The FlFFF-ICP-MS operating conditions are given in Table 1.

A UV/Visible spectrophotometer (Model V-530, Jasco, Easton, Maryland, USA) was used for acquisition of the UV/Visible absorption spectra of AgNPs, plasma protein, and protein-AgNPs association.

Chemicals

Bovine serum albumin (BSA) and tannic acid were purchased from Fluka (Buchs, Switzerland). γ- globulin and fibrinogen were purchased from Sigma–Aldrich (Steinheim, Germany). Silver nitrate, sodium azide and nitric acid (65%) were from Merck (Darmstadt, Germany). Tris (hydroxymethyl aminomethane) and FL-70® detergent (AR 98% assay) were from Fisher Scientific (Leicestershire, U.K.). De-ionized water (18.2 MΩ cm^{-1}) obtained from a water purification system (Barnstead International, Dubuque, IA, U.S.A.) was used throughout the experiment. All glassware was washed and soaked overnight in 30% HNO_3, and rinsed again with de-ionized water before use.

Two types of carrier liquid were used in the experiment. A 0.02% (w/v) FL-70 with 0.02% (w/v) sodium azide was used for size characterization of AgNPs. Another carrier liquid was a 30 mM tris (hydroxymethyl aminomethane), Tris, buffered at pH 9, which was used for investigation of AgNPs-plasma protein association.

Silver nanoparticles were prepared by using the method described by Sivaraman et al. [16]. While stirring, 25 mL of 0.3 mM tannic acid adjusted pH by K_2CO_3 and 5 mL of 3 mM silver nitrate were mixed in a conical flask. Three pH conditions were used, including pH of 8, 9, and 10 to prepare AgNPs of various sizes. A brown yellow solution appeared immediately, indicating the formation of tannic stabilized AgNPs. Albumin of 5.2 x 10^{-1} M, γ- globulin of 6.2 x 10^{-2} M, and fibrinogen of 5.8 x 10^{-3} M were prepared in Tris-buffer.

Calculation of AgNPs concentration

The concentration of the synthesized AgNPs was calculated by the method described by Mariam et al. [7]. By assuming that AgNPs are spherical in shape, the number of silver atoms was calculated by considering that the volume ratio of silver atom to AgNPs is 74.1% in the cubic structure. The radius of silver atom is 0.144 nm, and therefore its volume is 0.0125 nm^3. For AgNPs with the diameter of d nm, its volume is $(\pi/6)d^3$ nm^3. Thus, the number of silver atoms (N) in each AgNPs is equal to $\frac{74.1}{100} \times \frac{\pi}{6} \times d^3 \times \frac{1}{0.0125}$, which is calculated to be 31 d^3 [7]. The concentration of the AgNPs was then calculated by taking the ratio of the total number of silver atoms added to the reaction solution (N_{Total}) and the product between the number of silver atoms present in each nanoparticle (N) and the volume of the reaction solution in liters (V) and the Avogadro's constant (N_A). By assuming that all silver atoms were converted to AgNPs completely, therefore, the concentrations of various AgNPs

sizes of 2.6, 10, 23 nm were calculated to be 9.2 x 10^{-7}, 1.6 x 10^{-8}, 1.3 x 10^{-9} M, respectively. Calculations are given in the Supporting Information.

Observation of incubation time and concentration of AgNPs with plasma proteins

Two parameters influencing protein-nanoparticles association were investigated. These included the effects of incubation time and AgNPs concentration on protein binding. To examine the effect of incubation time, 2.6 nm tannic stabilized AgNPs of 4.6 x 10^{-7} M was incubated with either 2.6 x 10^{-1} M BSA, 3.1 x 10^{-2} M globulin, or 2.9 x 10^{-3} M fibrinogen at 37 °C for 5 min, 2, and 24 h. To examine the effect of AgNPs concentration on its binding with proteins, 2.6 nm tannic stabilized AgNPs of various concentrations as 9.2 x 10^{-8}, 2.7 x 10^{-7}, and 4.6 x 10^{-7} M were incubated with either 2.6 x 10^{-1} M bovine serum albumin, 3.1 x 10^{-2} M globulin, or 2.9 x 10^{-3} M fibrinogen at 37°C for 24 h. After incubation, the mixture was introduced into FlFFF for characterization. After fractionation, the effluent was directed through a UV detector and sequentially to ICP-MS.

Observation of stoichiometric binding between AgNPs and BSA

The stoichiometric binding between AgNPs with BSA was investigated by incubating different concentrations of bovine serum albumin with 2.6 nm tannic stabilized AgNPs of 9.2 x 10^{-8} M at 37 °C for 5 min. To confirm the stoichiometric binding between AgNPs with BSA, various concentrations of tannic stabilized AgNPs were incubated with BSA of 1.5 x 10^{-2} M. After incubation, the mixture was introduced into FlFFF-ICP-MS. The mole ratio between AgNPs and BSA was examined by keeping AgNPs and BSA constant as shown in Table 2 and 3, respectively.

Results and Discussion

Characterization of silver nanoparticles

Characterization of the synthesized AgNPs was performed using UV-visible absorption spectrophotometry and FlFFF. With UV-visible absorption spectrophotometry, the blank solution containing tannic acid at the same pH as the tannic stabilized AgNPs was filled in a reference cuvette for background subtraction. The absorption spectra of AgNPs displayed the surface plasmon resonance bands at 400, 410, and 420 nm for tannic stabilized AgNPs at pH 8, 9, and 10, respectively, as displayed in Figure 1a. These peaks indicated the formation of AgNPs. With FlFFF, the particle size distributions showed the peaks at 23.0 ± 0.2, 10.0 ± 0.3, and 2.6 ± 0.1 nm for tannic stabilized AgNPs at pH 9, 10, and 11, respectively, as illustrated in Figure 1b. The large void peaks observed in the fractograms shown in Figure 1b were due to the incomplete removal of the negatively charged tannic acid through the negatively charged cellulose acetate membrane during a very short time equilibration step (1.1 min, Table 1). The trends of particles sizes obtained from UV-visible absorption spectrophotometry and FlFFF were in good agreement. As can be seen, the smaller particles size of AgNPs exhibited plasmon resonance peak at shorter wavelength as compared to the bigger particle. These AgNPs were used in further experiments to observe the association between these particles and proteins.

As reported by other investigators [7, 17], the complex formation of BSA and AgNPs could be characterized by UV-visible absorption spectrophotometry. The absorption spectrum of BSA displayed a peak maximum at 278 nm (Figure 2). In the presence of AgNPs as illustrated in Figure 2a, 2b, 2c for AgNPs of 2.6, 10, and 23 nm, respectively, the absorbance at 278 nm of BSA increased with increasing in AgNPs concentrations, suggesting

the formation of the ground state complex between BSA and AgNPs [7]. The apparent association constant (K_{app}) for the complex formation between BSA and AgNPs was then calculated using the method reported by Benesi and Hildebrand [17], as illustrated in Figure 2d. The slope of the graph represents the reciprocal of K_{app} (A_c-A_0) and the intercept represents the reciprocal of (A_c-A_0), where A_c is the absorbance of the AgNPs-BSA complex and A_0 is the absorbance of BSA. Therefore, the values of K_{app} for AgNPs size of 2.6, 10, and 23 nm were calculated to be 5.2 x 10^7, 8.8 x 10^7, and 9.8 x 10^8 L mol^{-1}, respectively. This trend suggests that the bigger the particle size, the higher the value of the apparent association constant. The increase of the K_{app} value was found to linearly depend on the increase of the particle volume ($K_{app} \propto d^3$).

FlFFF-ICP-MS for observation of protein-AgNPs association

The effects of incubation time and AgNPs concentration on the binding of the protein to AgNPs were examined using FlFFF-ICP-MS. The proteins investigated were BSA, globulin, and fibrinogen. The particle size of AgNPs was 2.6 nm. In order to understand if the binding was due to the binding between the proteins and AgNPs, or the free dissolved Ag ions which were not converted into AgNPs, the remaining dissolved Ag ions were estimated. The estimation was performed by calculating the amount of Ag detected under the fractogram compared with the amount of Ag from AgNPs suspension, which was nebulized directly into the ICP-MS without flowing through the FlFFF channel. By taking into consideration that the sample recovery of AgNPs fractionation in the FlFFF channel was approximately 80%, the remaining dissolved Ag ion in the AgNPs were estimated to be approximately 5%. Therefore, the binding behavior discussed hereafter is mainly due to the binding between the protein and AgNPs.

Effect of incubation time

The fractograms of tannic stabilized AgNPs are illustrated in Figure 3a (with UV detection at 400 nm) and Figure 3b (with ICP-MS detection). Two peaks were observed in Figure 3a, by which the first peak (1.6 min) was assigned to the excess tannic acid whereas the second peak (4.8 min) was assigned to AgNPs, which was confirmed by one distinct peak at 5.5 min as observed in Figure 3b with ICP-MS detection. With UV detection, the large void peak was observed (1.6 min), owing to the incomplete removal of negatively charged tannic acid through the negatively charged cellulose acetate membrane during a 1.1 min equilibration step. No changes were observed upon incubation of this tannic acid stabilized AgNPs at 37 ℃ for 24 h. The fractograms of BSA are illustrated in Figure 3c (with UV detection at 280 nm) and Figure 3d (with ICP-MS detection). One distinct peak was observed at 3.4 min with UV detection (Figure 3c, red) and this was clearly the peak of BSA. No signal was observed with the ICP-MS detection (Figure 3d, red). Different incubation times at 5 min, 120 min, and 24 h were given to allow BSA to interact with AgNPs. For the mixture, the fractograms with varying incubation times are shown in Figure 3c (with UV detection at 280 nm) and Figure 3d (with ICP-MS detection). With ICP-MS detection, it was clearly seen that the peaks illustrating the signal of Ag were shifted from 5.5 min (Figure 3b) to approximately 3 min retention time (Figure 3d), indicating the interaction between AgNPs and BSA. The association between AgNPs and BSA can be the formation of a “nanoparticle-protein corona” which has been documented in many published articles [18, 19]. The formation of a "protein-corona" would affect the interactions with the membrane, resulting in shift of the retention times [14, 20]. Nonetheless, the formation of a “nanoparticle-protein corona” was unlikely as it should result in larger particle formation. Alternatively, the peak

at 3 min might be due to the binding between BSA with the released Ag ion from the AgNPs, as reported by other investigators [21].

As evidenced by Cedervall et al. [18], the nanoparticle-protein corona formation is a complex and time-dependent process, which is governed by thermodynamic and kinetic factors. Under the condition studied herein, the association between BSA and AgNPs or the released Ag ion from the AgNPs occurred within 5 min of incubation time. With longer incubation time at 24 h, bimodal characteristic was observed by the appearance of the peak at approximately 10 min, implying that AgNPs might grow bigger. The shift to bigger size may either be caused by three reasons. The first plausible reason is due to the nanoparticle-protein corona formation, yielding larger particle size. The second plausible reason is due to the displacement of tannic acid stabilizing agent with BSA, which is more steric leading to larger particle size. The displacement of stabilizing agent with BSA might occur through the ligand-exchange or place-exchange reaction as reported by the other investigators for AuNPs [22]. The third plausible reason is due to the interaction between tannic acid and BSA as the association between tannic acid and proteins has been widely known by food scientists to cause astringency perception [23].

To demonstrate the effect of incubation time on AgNPs binding with globulin, the fractograms as shown in Figures 3e and 3f are considered. The fractograms of globulin are illustrated in Figure 3e (with UV detection at 280 nm) and Figure 3f (with ICP-MS detection). With UV detection (Figure 3e, red), the peak of globulin appeared at retention time of 6.2 min with a shoulder at 8.7 min. Clearly, no signal was observed with the ICP-MS detection (Figure 3f, red). Different incubation times at 5 min, 120 min, and 24 h were given to allow globulin to interact with AgNPs. For the mixture, the fractograms with varying incubation times are shown in Figure 3e (with UV detection at 280 nm) and Figure 3f (with ICP-MS detection). At incubation times of 5 and 120 min, monomodal distribution was

observed at the retention time of 13.2 min. It is interesting to note that the peak at 13.2 min shifted significantly from the peak of individual AgNPs at 5.5 min (Figure 3b), suggesting the rapid occurrence of the binding between AgNPs and globulin. This globulin-AgNPs corona formation resulted in larger particle size. Alternatively, the peak at 13.2 min might be assigned to the binding between the released Ag ion with the dimeric form of globulin as the monomeric form of globulin displayed a peak at approximately 6.2 min (Figure 3e). One might wonder why this dimeric peak was not distinct with the absorbance detection at 280 nm, as shown in Figure 3e. We believed that the dimeric form was present in a relatively lower concentration than the monomeric form of globulin. Nonetheless, the released Ag ion from AgNPs showed preferential association with the globulin dimer, leading to the more distinct peak of the dimeric form when ICP-MS was used for silver detection. The dimerization of globulin on the AgNPs surface might be caused by structural perturbation of globulin by the high surface-to-volume ratios of nanoparticles, which resulted in high concentration of globulin adsorbed at the particle surface of low dimensionality, enhancing the probability of partial unfolding of globulin, as described by Linse et al [24]. Nonetheless, bimodal distribution was observed when the incubation time reached 24 h, by displaying peaks at 6.6 and 13.2 min. This suggested that in our experiment the dimerization occurred rapidly within 5 min and was found reversible as the monomeric peak at 6.6 min retention time was observed at the incubation time of 24 h. Alternatively, the peak at 6.6 nm might be due to binding of the released Ag ion from AgNPs with the monomeric fraction.

The effect of incubation time on the binding of AgNPs to fibrinogen was examined, as illustrated in Figures 3g and 3h. The fractograms of fibrinogen are illustrated in Figure 3g (with UV detection at 280 nm) and Figure 3h (with ICP-MS detection). With UV detection (Figure 3g, red), the peak of fibrinogen appeared at retention time of 10.3 min. As expected, no signal was observed with the ICP-MS detection (Figure 3h, red). Fibrinogen was allowed

to incubate with AgNPs for various incubation times at 5 min, 120 min, and 24 h. Comparing between Figure 3g and Figure 3h, the peak positions were not similar, suggesting that AgNPs were preferentially associated to the larger molecular weight fibrinogen. Considering Figure 3h, the binding occurred within 5 min of incubation time, as can be observed from the peak at 14.5 min, which slightly shifted toward larger size than the pure fibrinogen.

Effect of AgNPs concentration

To examine the effect of AgNPs concentration on the association between BSA and AgNPs, various concentrations of AgNPs were incubated with BSA at fixed time of 24 h. With increased concentration of AgNPs, the signal intensity was increased, suggesting that more AgNPs could be associated with BSA. The shoulder peak at around 10 min was observed when the concentration of AgNPs increased up to 4.9×10^{-7} M, suggesting that the enlargement of the particles depends on the concentration of AgNPs. The nanoparticle-protein corona formation, or the place-exchange reaction between BSA and tannic acid or the association between BSA and tannic acid was not taken place when the concentration of AgNPs was too low.

The binding of globulin to AgNPs with various AgNPs concentrations was also examined at a fixed incubation time of 24 h. When concentration of AgNPs was increased, the signal intensity of fractogram was increased. Broad distribution was observed at low concentration of globulin. The distribution became bimodal showing distinct peaks at 6.6 and 13.2 min retention time when the concentration of AgNPs was increased to 4.6×10^{-7} M. This suggests that the dimerization of globulin induced by AgNPs is concentration dependent.

The binding of fibrinogen to AgNPs with various AgNPs concentrations is shown in Figure 4e and Figure 4f. With AgNPs of 9.2×10^{-8} M, the signal of Ag was quite negligible

suggesting that this concentration might be too low to cause the binding with 2.9 x 10^{-3} M fibrinogen (Figure 4f). However, when the concentration of AgNPs increased to 2.7 x 10^{-7} M, the peak was observed at 16.6 min. Formation of nanoparticle-protein corona between AgNPs and fibrinogen is possible as reported by Cedervall et al [18]. With increasing AgNPs to 4.6 x 10^{-7} M, bimodal characteristic was observed at 10.5 and 14.2 min. The peak at 10.5 min is quite close to the peak of pure fibrinogen, suggesting the possible occurrence of fibrinogen binding with the released Ag ion from the AgNPs.

Binding stoichiometry between AgNPs and BSA

This is the first time that FlFFF-ICP-MS was applied to examine the stoichiometry of the binding of BSA with AgNPs. Various concentrations of BSA were incubated with AgNPs of 9.2 x 10^{-8} M. In order to differentiate the signal of Ag between the Ag binding to BSA and the Ag in the AgNPs, the fractogram of the mixture between BSA and AgNPs (Figure 5a) was deconvoluted using PeakFit® program (an automated peak separation analysis software). The deconvoluted peaks of the fractogram are illustrated in Figure 5b, which showed two distinct peaks at 3.6 and 5.9 min. The first peak was related to BSA binding and the second peak was contributed from AgNPs. The area under the first deconvoluted peak (peak I) of the Ag fractogram was observed. Using the mole-ratio method, the peak area under the first deconvoluted peak (peak I) of the Ag fractograms obtained from varying concentrations of BSA was plotted as a function of BSA concentration as illustrated in Figure 5c. At low concentration of BSA, the peak area of the first deconvoluted peak (peak I) of Ag fractogram was low and the peak area increased rapidly with increasing in BSA concentration from 7.46 x 10^{-2} to 1.49 x 10^{-1} M. After this point, the peak area under the first deconvoluted peak (peak I) of the Ag fractogram became relatively

constant with increasing BSA, suggesting that the binding became constant. The stoichiometric binding between BSA and AgNPs was determined at the inflection point or the point where the two straight lines met, which was at the BSA concentration of 1.49×10^{-1} M, implying that the binding ratio between BSA and AgNPs was $1 : 6.2 \times 10^{-7}$. This is only a rough estimation as the increment of the concentration from 7.46×10^{-2} to 1.49×10^{-1} M was rather unrefined.

To confirm the stoichiometric binding between AgNPs and BSA, similar experiment was performed by varying AgNPs concentrations with fixed BSA concentration at 1.49×10^{-2} M. For very low concentrations of AgNPs, no signal of Ag was observed at the peak of BSA. Until at AgNPs of 7.4×10^{-9} M, the signal of Ag increased significantly and became relatively constant thereafter (Figure 5d). This suggests that the stoichiometric binding of BSA and AgNPs is $1 : 4.9 \times 10^{-7}$. Using the mole ratio method by keeping either AgNPs or BSA constant, the ratio of BSA and AgNPs were found to be approximately $1 : 5 \times 10^{-7}$, suggesting that approximately 2×10^{6} molecules of BSA adsorbed on a single AgNP with the size of 2.6 nm.

Conclusions

With the use of UV-visible spectrophotometry, complex formation of BSA and AgNPs could be observed and the apparent association constant (K_{app}) could be determined as reported by other investigators [7, 17]. The novel finding from this study, however, is that the K_{app} value was found to linearly depend on the particle volume ($K_{app} \propto d^3$). Furthermore, FlFFF-ICP-MS was demonstrated as an alternative method to monitor the protein-AgNPs association. Plasma proteins (BSA, globulin, and fibrinogen) were investigated for their formation of protein corona with AgNPs. The interaction between BSA and AgNPs was

affected by both incubation time and concentration of AgNPs. The binding of plasma protein and AgNPs occurred rapidly within 5 min of incubation time. Additionally, the investigation of the stoichiometric binding between BSA and AgNPs was possible by FlFFF-ICP-MS, showing potential applications of the technique to study the complexation between other metals and macromolecules.

Acknowledgements

We sincerely thank the Office of the Higher Education Commission, Ministry of Education, Thailand through the Center for Innovation in Chemistry: Postgraduate Education and Research Program in Chemistry (PERCH-CIC) for the scholarship given to PW and funding for equipment. Financial supports from the Thailand Research Fund (TRF) and Mahidol University under the National Research Universities Initiative are gratefully acknowledged. Thanks are also due to the useful comments from anonymous reviewers.

References

1. C.-F. Chau, S.-H. Wu and G.-C. Yen, *Trends Food Sci. Tech.*, 2007, **18**, 269-280.
2. Y. Li, Y. Zhang and B. Yan, *Int. J. Mol. Sci.*, 2014, **15**, 3671-3697.
3. Y. Teow, P. V. Asharani, M. P. Hande and S. Valiyaveettil, *Chem. Commun.*, 2011, **47**, 7025-7038.
4. S. Elodie, D. Julien, R.-L. Fernando and D. Jean-Marie, *J. Phys. Conf. Ser.*, 2011, **304**, 012039.
5. C. Beer, R. Foldbjerg, Y. Hayashi, D. S. Sutherland and H. Autrup, *Toxicol. Lett.*, 2012, **208**, 286-292.
6. L. Li, Q. Mu, B. Zhang and B. Yan, *Analyst*, 2010, **135**, 1519-1530.
7. J. Mariam, P. M. Dongre and D. C. Kothari, *J. Fluoresc.*, 2011, **21**, 2193-2199.

8. M. A. Dobrovolskaia, A. K. Patri, J. Zheng, J. D. Clogston, N. Ayub, P. Aggarwal, B. W. Neun, J. B. Hall and S. E. McNeil, *Nanomed.-Nanotechnol.*, 2009, **5**, 106-117.
9. Z. J. Deng, G. Mortimer, T. Schiller, A. Musumeci, D. Martin and R. F. Minchin, *Nanotechnology*, 2009, **20**.
10. I. Lynch and K. A. Dawson, *Nano Today*, 2008, **3**, 40-47.
11. A. R. Poda, A. J. Bednar, A. J. Kennedy, A. Harmon, M. Hull, D. M. Mitrano, J. F. Ranville and J. Steevens, *J. Chromatogr. A*, 2011, **1218**, 4219-4225.
12. J. G. Coleman, A. J. Kennedy, A. J. Bednar, J. F. Ranville, J. G. Laird, A. R. Harmon, C. A. Hayes, E. P. Gray, C. P. Higgins, G. Lotufo and J. A. Steevens, *Environ. Toxicol. Chem.*, 2013, **32**, 2069-2077.
13. A. R. Poda, A. J. Kennedy, M. F. Cuddy and A. J. Bednar, *J. Nanopart. Res.*, 2013, **15**, 1-10.
14. K. Loeschner, J. Navratilova, C. Købler, K. Mølhave, S. Wagner, F. von der Kammer and E. H. Larsen, *Anal. Bioanal. Chem.*, 2013, **405**, 8185-8195.
15. E. Bolea, J. Jimenez-Lamana, F. Laborda, I. Abad-Alvaro, C. Blade, L. Arola and J. R. Castillo, *Analyst*, 2014, **139**, 914-922.
16. S. K. Sivaraman, I. Elango, S. Kumar and V. Santhanam, *Curr. Sci.*, 2009, **97**, 1055-1059.
17. H. A. Benesi and J. H. Hildebrand, *J. Am. Chem. Soc.*, 1949, **71**, 2703-2707.
18. T. Cedervall, I. Lynch, S. Lindman, T. Berggård, E. Thulin, H. Nilsson, K. A. Dawson and S. Linse, *P. Natl. Acad. Sci. USA*, 2007, **104**, 2050-2055.
19. A. L. Capriotti, G. Caracciolo, C. Cavaliere, V. Colapicchioni, S. Piovesana, D. Pozzi and A. Laganà, *Chromatographia*, 2014, **77**, 755-769.
20. A. Ulrich, S. Losert, N. Bendixen, A. Al-Kattan, H. Hagendorfer, B. Nowack, C. Adlhart, J. Ebert, M. Lattuada and K. Hungerbühler, *J. Anal. At. Spectrom.*, 2012, **27**, 1120-1130.
21. A-K. Ostermeyer, C. K. Mumuper, L. Semprini and T. Radniecki, Environ. Sci. Technol., 2013, **47**, 14403-14410.
22. R. Sardar, J. W. Park and J. S. Shumaker-Parry, *Langmuir*, 2007, **23**, 11883-11889.
23. E. Obreque-Slier, C. Mateluna, A. Peña-Neira and R. López-Solís, *J. Agric. Food. Chem.*, 2010, **58**, 8375-8379.
24. S. Linse, C. Cabaleiro-Lago, W. F. Xue, I. Lynch, S. Lindman, E. Thulin, S. E. Radford and K. A. Dawson, *P. Natl. Acad. Sci. USA*, 2007, **104**, 8691-8696.

Table 1 FlFFF-ICP-MS operating conditions

FlFFF: Model PN-1021-FO	
Channel flow rate/mL min^{-1}	1.0
Cross flow rate/mL min^{-1}	2.0
Equilibration time/min	1.1
Carrier liquid	30 mM Tris-HNO_3 (buffered at pH 9)
Membrane	1 kDa MWCO, poly(regenerated cellulose acetate)
ICP-MS: Sciex/Elan 6000 Perkin Elmer	
RF generator frequency/MHz	40
RF power/W	1100-1300
Nebulizer gas flow rate/L min^{-1}	0.90-0.95
Coolant gas flow rate/L min^{-1}	15.0
Auxiliary gas flow rate/L min^{-1}	0.90
Mode	Peak hopping
Dwell time/measurement/isotope	25
Torch	Fassel type
Torch injector	Ceramic alumina
Spray chamber	Ryton®Scott-type
Nebulizer	Gem-tip® cross flow
Isotopes monitored	^{107}Ag, ^{109}Ag

Table 2 Mole ratio method for determination of stoichiometric binding between BSA and AgNPs. The concentration of AgNPs was kept constant.

Concentration of AgNPs (M)	Concentration of BSA (M)
9.2×10^{-8}	1.49×10^{-2}
	7.46×10^{-2}
	1.49×10^{-1}
	1.79×10^{-1}
	2.08×10^{-1}
	2.38×10^{-1}
	2.98×10^{-1}

Table 3 Mole ratio method for determination of stoichiometric binding between BSA and AgNPs. The concentration of BSA was kept constant.

Concentration of BSA (M)	Concentration of AgNPs (M)
1.49×10^{-2}	1.84×10^{-9}
	3.68×10^{-9}
	4.60×10^{-9}
	5.52×10^{-9}
	5.98×10^{-9}
	6.44×10^{-9}
	7.36×10^{-9}
	8.28×10^{-9}
	9.20×10^{-9}
	1.10×10^{-8}

Figure Captions

Figure 1 (a) UV-visible absorption spectra and (b) fractograms of tannic stabilized AgNPs synthesized at pH 8 (blue), 9 (green), 10 (red).

Figure 2 UV-visible absorption spectra of 2.6 x 10^{-1} M BSA (black) and BSA in the presence of AgNPs of (a) 2.6 nm with the concentration of 9.2 x 10^{-8} M (blue), 2.7 x 10^{-7} M (green), and 4.6 x 10^{-7} M (red); (b) 10 nm with the concentration of 1.6 x 10^{-9} M (blue), 4.8 x 10^{-9} M (green), and 8.0 x 10^{-9} M (red); and (c) 23 nm with the concentration of 1.3 x 10^{-10} M (blue), 3.9 x 10^{-10} M (green), and 6.5 x 10^{-10} M (red). [Note – increasing concentration of AgNPs resulted in higher absorbance] (d) Linear plots for calculation of K_{app} between BSA and AgNPs of 2.6 nm (○), 10 nm (△), and 23 nm (□).

Figure 3 Fractogram of 2.6 nm tannic stabilized AgNPs 4.6 x 10^{-7} M: (a) with UV detection; and (b) with ICP-MS detection. Fractograms of BSA 2.6 x 10^{-1} M (c and d, red); globulin 3.1 x 10^{-2} M (e and f, red); fibrinogen 2.9 x 10^{-3} M (g and h, red), mixed with 2.6 nm tannic stabilized AgNPs 4.6 x 10^{-7} M: (c,e,g) with UV detection; and (d,f,h) with ICP-MS detection, at various incubation times of 5 min (green), 120 min (blue), and (brown) 24 h.

Figure 4 Fractograms of 2.6 x 10^{-1} M BSA (a and b, red); 3.1 x 10^{-2} M globulin (c and d, red); 2.9 x 10^{-3} M fibrinogen (e and f, red), incubated 24 h with 2.6 nm tannic stabilized AgNPs of various concentrations as (green) 9.2 x 10^{-8}; (blue) 2.7 x 10^{-7}; and (brown) 4.6 x 10^{-7} M: (a,c,e) with UV detection; and (b,d,f) with ICP-MS detection.

Figure 5 (a) Fractogram of the mixture between 1.49 x 10^{-2} M BSA and 9.2 x 10^{-8} M AgNPs, with ICP-MS detection. (b) The deconvoluted peaks of the fractogram, showing two peaks (Peak I, blue and Peak II, red). Plots of peak area under the deconvoluted peak I of the Ag fractograms versus concentrations of (c) BSA when the concentration of AgNPs was 9.2 x 10^{-8} M, and (d) AgNPs when the concentration of BSA was 1.49 x 10^{-2} M.

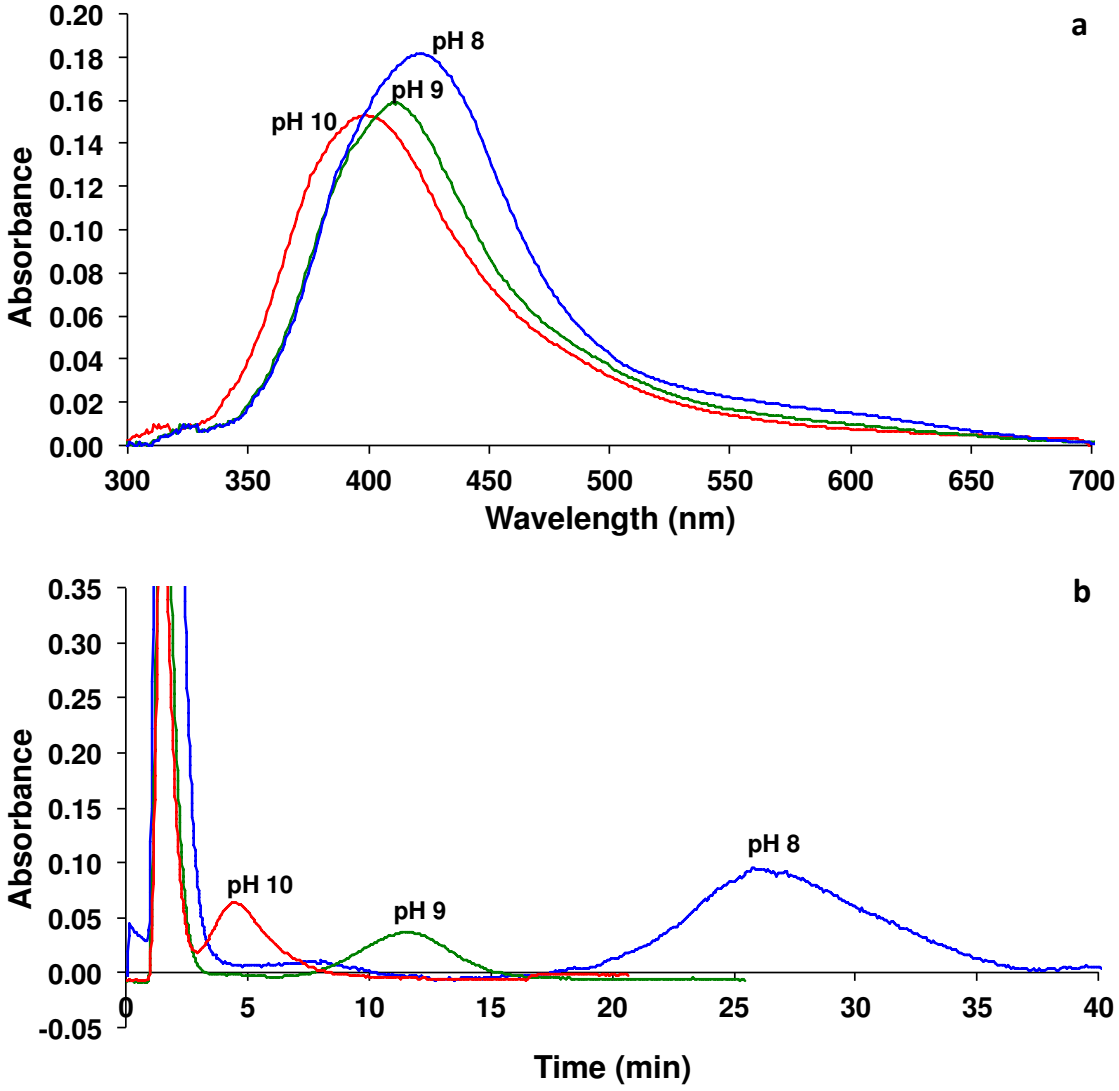

Figure 1

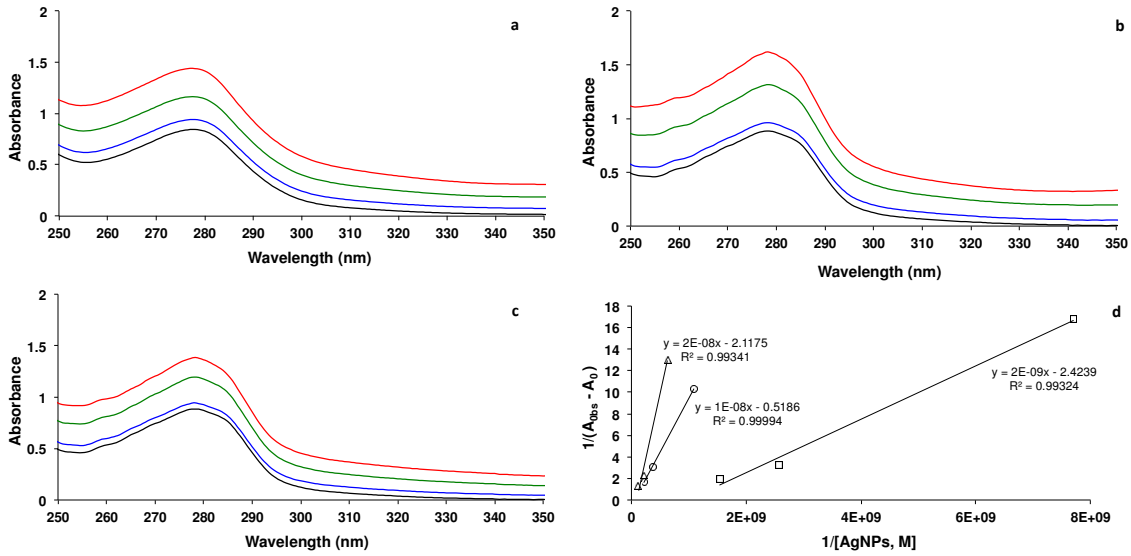

Figure 2

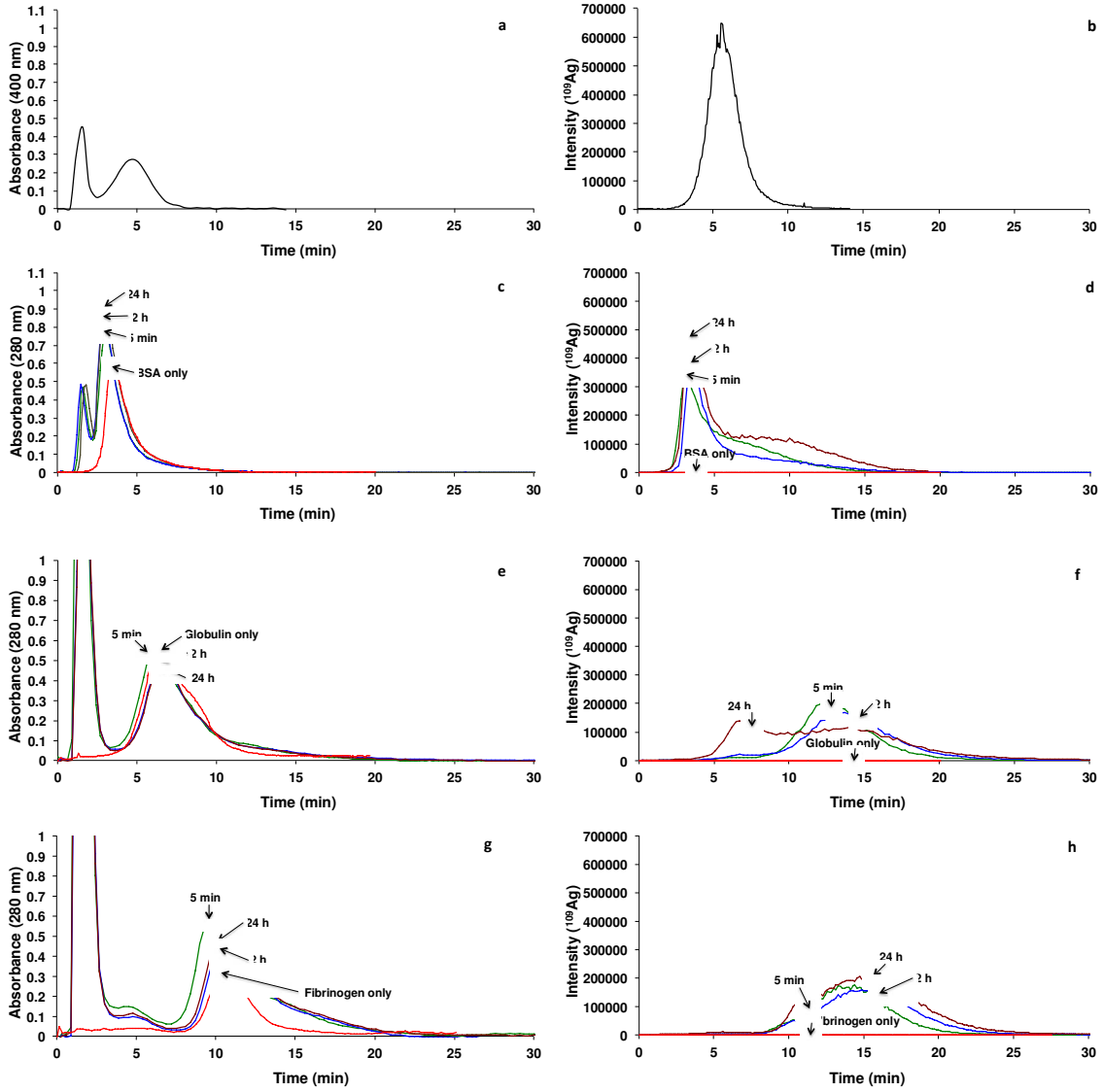

Figure 3

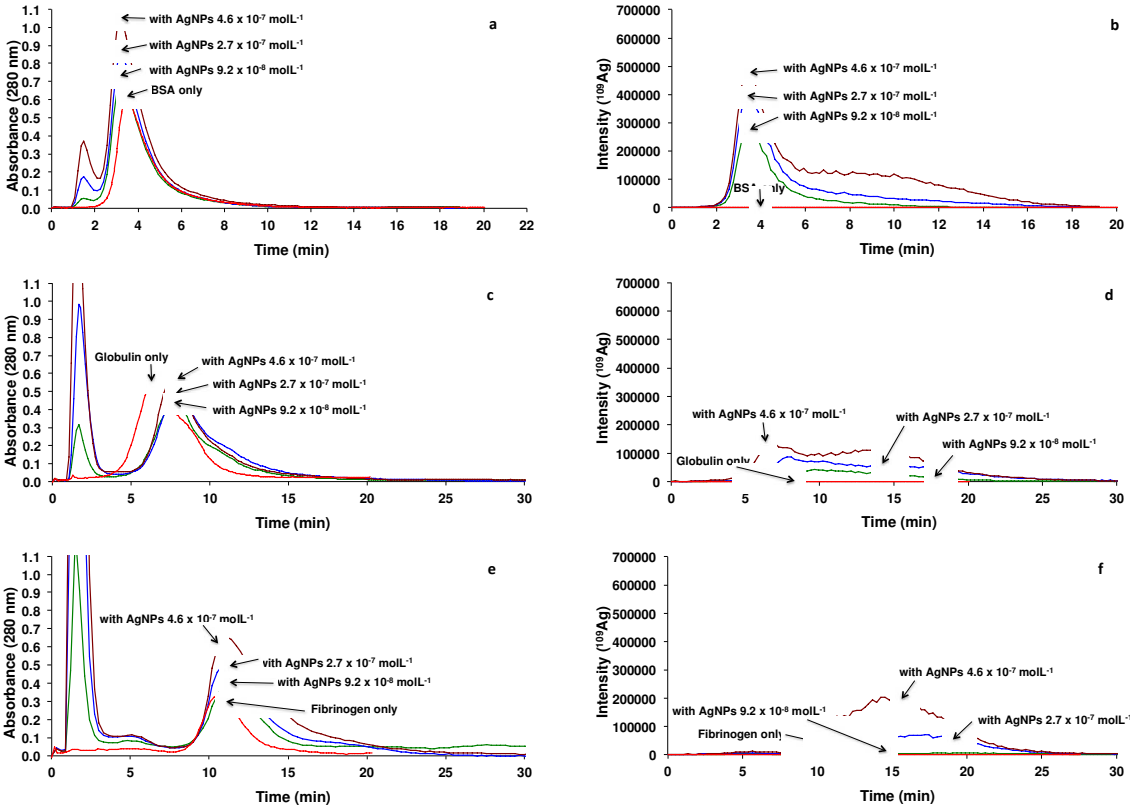

Figure 4

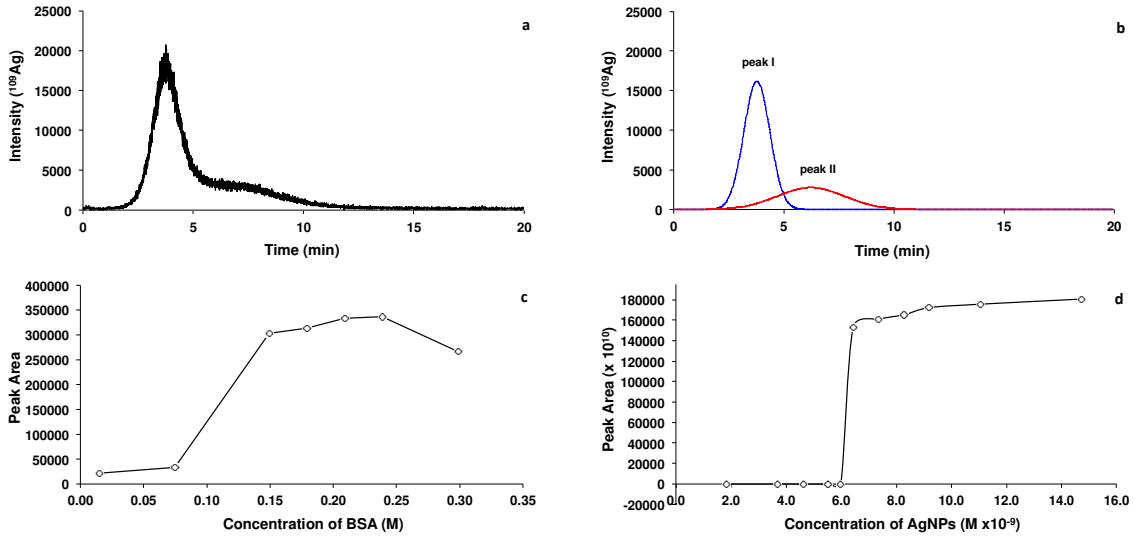

Figure 5